

Bubble Dynamics Induced by Pulsed-Laser Evaporation of Ink as a Method to Develop Novel Print Heads

Deoksuk Jang, Jonggan Hong and Dongsik Kim

Department of Mechanical Engineering, POSTECH, Pohang 790-784, Korea

E-mail: dskim87@postech.ac.kr

Sung-Hoon Choa

MEMS Lab., Samsung Advanced Institute of Technology, Yongin 449-712, Korea

Abstract. *The bubble dynamics induced by direct laser heating is experimentally analyzed as a first step to assess the technical feasibility of laser-based ink jet technology. To understand the interaction between laser light and ink, the absorption spectrum is measured for various ink colors and concentrations. The hydrodynamics of laser-generated bubbles is examined by laser flash photography. When an Ar ion laser pulse (wavelength 488 nm) with an output power up to 600 mW is incident on the ink solution through a transparent window, a hemispherical bubble with a diameter up to $\sim 100 \mu\text{m}$ can be formed with a lifetime in the range $\sim O(10 \mu\text{s})$ depending on the laser power and the focal-spot size. A parametric study has been performed to reveal the effect of laser pulse width, output power, ink concentration, and color on the bubble dynamics. The results show that the bubble generated by a laser pulse is largely similar to that produced by a thin film heater. Consequently, the present work demonstrates the feasibility of developing a laser-actuated droplet generation mechanism for applications in ink jet print heads. Furthermore, the results of this work indicate that the droplet generation frequency is likely to be further increased by optimizing the process parameters. © 2006 Society for Imaging Science and Technology.*

[DOI: 10.2352/J.ImagingSci.Technol.(2006)50:2(173)]

INTRODUCTION

In drop-on-demand ink jet printers, thin film resistors are commonly used as pressure generators to eject picoliter scale ink droplets. Though the droplet generation method using thin film heaters is widely used in thermal ink jet print heads owing to a variety of advantages, the conventional droplet generation technology has several serious limitations which have to be overcome to meet the requirement of today's digital printing technology. One of the limitations is the speed performance of a printing unit. The operation frequency of a thermal ink jet print head is limited by the thermal time constant required for the relatively large heat-affected volume to cool down to its original state. Common piezoelectric print heads have similar speed performance because of the inertia of the moving structure. Therefore, several novel concepts based on optical heating of ink have been suggested to minimize the cooling time by reducing the thermal inertia and thus to enable higher repetition operation of ink jet devices.¹⁻⁷ Among the newly suggested con-

cepts, this work is concerned with a droplet generation mechanism that utilizes explosive vaporization and bubble generation by direct laser irradiation onto the printing ink. The main idea of the novel mechanism is to directly heat the ink by a laser pulse, eliminating the chance of temperature increase in the heating element.

While the bubble dynamics induced by a thin film heater has been thoroughly investigated both theoretically and experimentally,⁸⁻¹⁰ the phenomena associated with laser heating are hardly known. Though there have been some studies on high power laser interaction with liquids at a power density above or close to the plasma ignition threshold,¹¹⁻¹⁶ no investigation has been carried out to observe the laser-induced bubble dynamics in the explosive vaporization of absorbing liquid in the range of power density $O(10^4 \text{ W/cm}^2) \sim O(10^5 \text{ W/cm}^2)$, which corresponds to typical operating conditions of thermal ink jet printers. Consequently, this work studies the bubble dynamics in boiling under pulsed laser heating for examining the technical feasibility of the newly suggested concept. Ink solutions are heated by an Ar ion laser beam through a transparent window and the growth of the optically generated bubble is visualized by the laser flash photography with a time resolution of a few nanoseconds. The kinetics of bubble growth is analyzed based on the experimental observation by varying the process parameters such as the laser pulse width, power, and ink concentration.

CONCEPT OF LASER ACTUATED PRINT HEADS AND SCOPE OF THIS WORK

Ink droplets can be generated by laser irradiation, so called by the "photohydraulic" effect, via several different physical mechanisms. For example, surface vaporization, explosive vaporization with bubble generation, thermal expansion of the heated liquid, thermoelastic stress generation, and/or spallation can lead to ink droplet generation. Among the photohydraulic phenomena that may be applied to development of a novel laser actuated print head, this work is focused on the bubble dynamics that are produced by direct laser heating of ink and subsequent explosive vaporization. Figure 1 depicts the idea of a laser actuated bubble jet mechanism. In this concept, the thin film heater has been

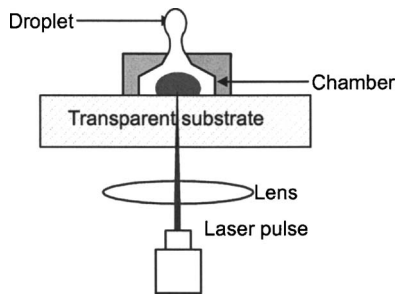


Figure 1. Concept of droplet ejection by direct laser heating of absorbing liquid in a chamber.

Table I. Advantages of laser actuated print heads and technical barriers.

Advantages	Technical barriers
<ul style="list-style-type: none"> • High speed printing due to rapid response (reduced thermal mass) 	Ink dependency (stability and property)
<ul style="list-style-type: none"> • Simple head structure (no buried heating element) 	High cost of laser source (feasibility of using a laser diode unknown)
<ul style="list-style-type: none"> • Array structure easily built 	Laser beam delivery system currently unavailable
<ul style="list-style-type: none"> • Nonthermal actuation possible by photomechanical effects 	Flimsy physical understanding
<ul style="list-style-type: none"> • High printing resolution 	
<ul style="list-style-type: none"> • Special printing possible (e.g., high-viscosity light hardening ink) 	
<ul style="list-style-type: none"> • Capillary-free structure possible (no special requirement in ink quality) 	
<ul style="list-style-type: none"> • No damage-sensitive thin film circuit potential to control cavitation damage by adjusting the bubble location 	
<ul style="list-style-type: none"> • No driving circuit or ASIC(application specific integrated circuit) required on the head area 	

replaced by a light source and beam delivery elements for direct heating of the liquid. The novel droplet generation concept based on direct heating of ink has several advantages over the conventional technique utilizing a thin film heater while there are also technical barriers to product development, as summarized in Table I. Among the advantages, such critical factors as printing speed, resolution, and chance of cavitation damage are directly related to the hydrodynamic phenomena in laser bubble generation. Furthermore, the cost effectiveness, as one of the most challenging technical barriers to successful application of this concept, is strongly correlated with the conversion efficiency from electromagnetic to mechanical energy in the bubble generation process. Therefore, solid understanding of the bubble dynamics is the key to further development of the concept for industrial applications.

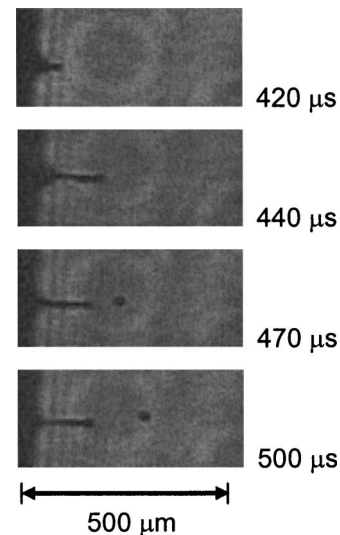


Figure 2. Images showing droplet ejection from a thin liquid film by pulsed laser heating (laser power: 610 mW, pulse width: 370 μs).

It is noted that a simple droplet generation test similar to that displayed in Fig. 1 is not sufficient to yield all the detailed information for developing a novel laser actuated print head. As there are many unknown parameters regarding the beam source and delivery scheme, including the beam spot size and the location of the focal plane, the droplet generation process can hardly be optimized by the test. Also, the results of our preliminary experiment on droplet generation indicate that the droplet size and the time required for droplet ejection are critically dependent on various experimental parameters, such as the geometry of the liquid chamber, the location of the laser focal point and laser fluence. Figure 2 shows an example of droplet generation from a thin liquid film. In this experiment, an ink layer of thickness 150 μm was formed by capillary pumping on a glass substrate and the layer was irradiated by an Ar ion laser pulse from the back surface through the glass substrate. In this experiment, it has been found that the liquid film thickness as well as the laser spot size or focal point changes the droplet generation characteristics significantly. Consequently, this work analyzes the bubble dynamics in bulk liquid without the ink chamber, i.e., without droplet ejection, to eliminate the complexity introduced by the geometry of the chamber. Development of a novel print head thus requires further work to elucidate the mechanisms of droplet formation from an ink chamber. To our knowledge, however, this work reports for the first time the results of dynamics of a laser produced bubble in the heat flux range relevant to ink jet printing technology.

LASER BEAM ABSORPTION BY INK

To examine the light-absorption properties of the color inks, the absorption-spectrum is measured for several ink colors and concentrations. Commercially available ink jet printer inks (JETRON KOREA LTD.), whose colors are magenta, cyan, yellow and black, were utilized in the experiment. The experimental setup for the absorption-spectrum measure-

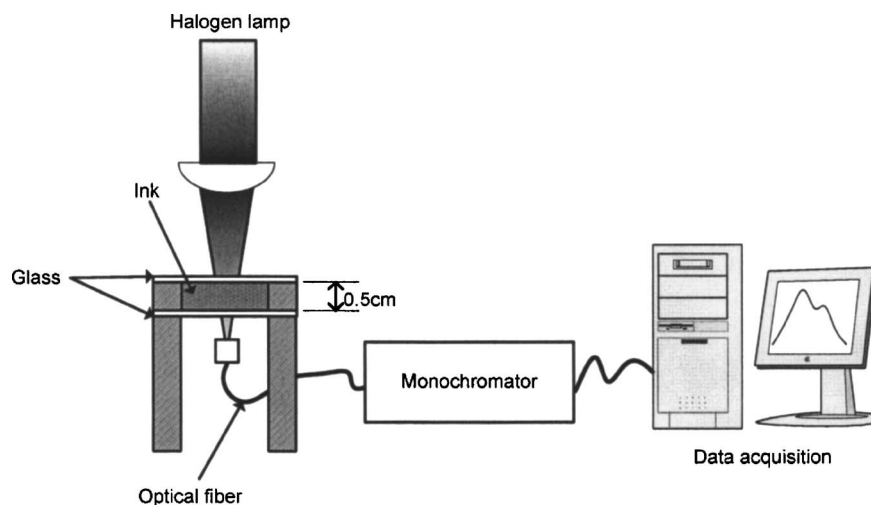


Figure 3. Schematic diagram of experimental setup for absorption spectrum measurement.

ment is displayed in Fig. 3. A glass cell containing the absorbing ink is exposed to the light from a halogen lamp at a normal incidence angle. The light emitted from the lamp is in the wavelength range from 400 to 850 nm. Since the light is absorbed by the ink solution, the light intensity drops after the test cell. The absorption spectrum of the transmitted light is measured and compared with a reference spectrum that is obtained using a reference glass cell without the ink. Comparison of the two signals yields the absorbance spectrum as shown in Fig. 4. While the black ink absorbs all wavelengths [from visible to near infrared (IR)], yellow ink shows strong absorption only in the wavelength range from 400 to 500 nm. Figure 4 reveals that complete absorption occurs in the 400–500 nm range for all colors. These results suggest that visible laser lines, e.g., Ar ion laser lines (488 nm) as in the present work, may be used for directly generating bubbles without introducing an additional light absorbing structure, like an absorbing thin metal film. It is noted that the absorption spectrum in Fig. 4 does not quantify the absorption coefficient as it was obtained using a 0.5 cm thick glass cuvette. Therefore, a similar experiment was performed to measure the linear absorption coefficient κ of the aqueous solutions of the ink precisely at the wavelength of the Ar ion laser. In this experiment, a thin test cell of thickness 150 μm was used to increase the intensity of the transmitted signal. The measured absorption coefficients of the ink solutions at 488 nm are 1.04×10^4 and $1.10 \times 10^4 \text{ m}^{-1}$ for 25% and 33% (by volume ink concentration), respectively.

EXPERIMENTAL SETUP FOR VISUALIZATION OF BUBBLE DYNAMICS

To investigate the hydrodynamics of laser generated bubbles, the laser flash photography experiment was performed as shown in Fig. 5. Bubbles were produced in the mixtures of commercial inks and deionized water and the behavior visualized by the fast photography technique. To heat the solution, an Ar ion laser (wavelength: 488 nm, variable pulse width: 10–100 μs) beam was focused onto the interface between the solution and a transparent quartz window. At dif-

ferent incident laser powers (100–610 mW), the pulse width was varied by an A/O (acousto-optic) modulator up to hundreds of microseconds. The laser beam has a Gaussian intensity distribution and is focused by a focusing lens of focal length 50 mm. The corresponding focal spot size (diameter) is estimated to be 26 μm . The bubbles were visualized by the standard laser flash shadowgraphy technique.¹¹ In the method, time resolved images of a bubble are captured by controlling the delay time between the pump (Ar ion laser) and the probe lasers [N_2 -pumped dye laser, $\lambda = 640$ or 440 nm, full width at half maximum (FWHM): 3 ns]. Accordingly, this visualization method captures only one image frame per pulse and the accuracy relies on the reproducibility of the experiment. At this point, another important limitation of the experimental technique needs to be pointed out. The laser flash photography method employed in this work requires transmission of a visible laser pulse. Even though the ink should be strongly absorbing to fulfill the condition of explosive bubble generation, the ink had to be diluted to allow minimum transmission of the probe laser beam. Consequently, aqueous solutions of the ink at concentrations lower than 50% by volume were used to observe the dynamics of the laser-produced bubble. It is noted that dilution of the ink decreases the laser absorbance and thus degrades the efficiency of the optical bubble generation process. The effect of ink concentration on the results of the analysis will later be described in detail.

DYNAMICS OF LASER GENERATED BUBBLE

When the laser pulse is incident on a magenta ink solution, a hemispherical bubble starts to expand after a certain characteristic time, i.e., the boiling incipience time or time to explosive bubble formation τ . It is obvious that this time scale as well as the cooling time determines the frequency of bubble generation. The dynamics of a typical laser generated bubble are displayed in Fig. 6 for a volume concentration of 33%. If the laser pulse width is shorter than τ , expansion of a hemispherical bubble ($\sim 100 \mu\text{m}$ in diameter) is not observed. Even in this case, small bubbles are generated at the interface and disappear immediately after laser beam is cut-

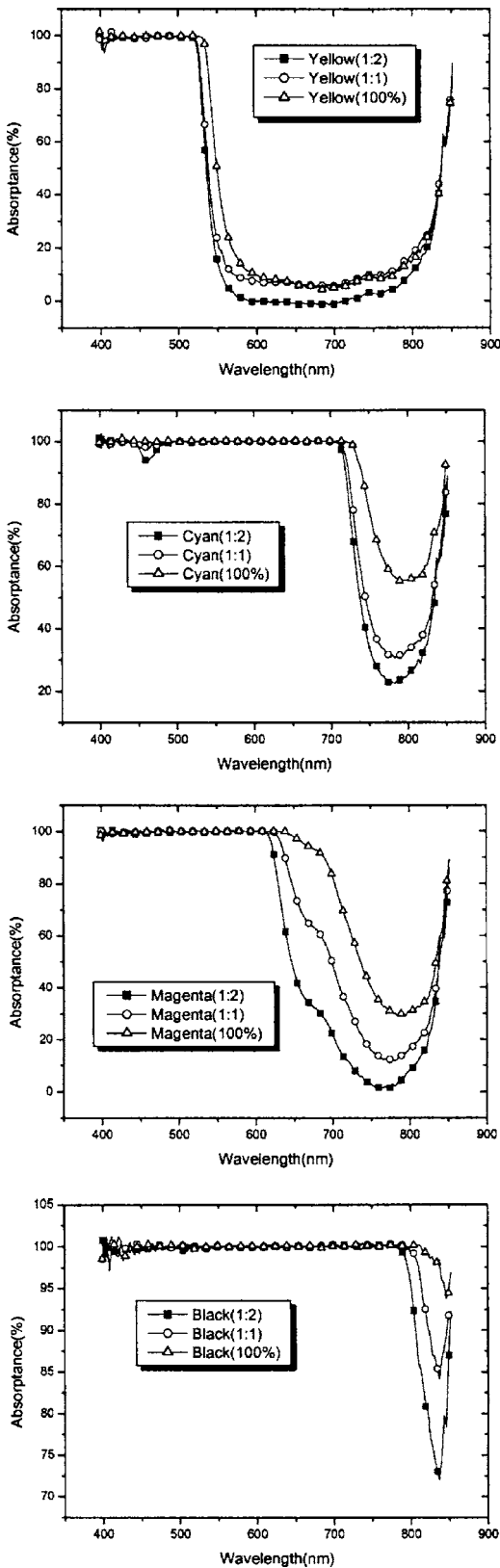


Figure 4. Transmission spectrum for various ink colors and concentrations.

off, without forming a relatively large and rapidly growing bubble. Figure 7 shows the variation of bubble volume with time for a laser pulse width of 9 μs. In this figure, the data

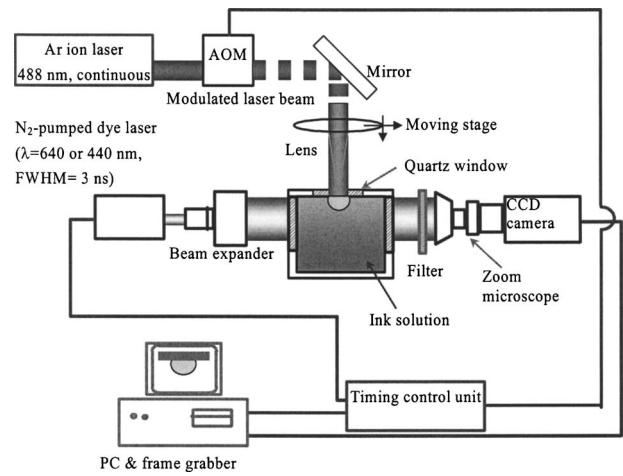


Figure 5. Experimental setup for fast photography.

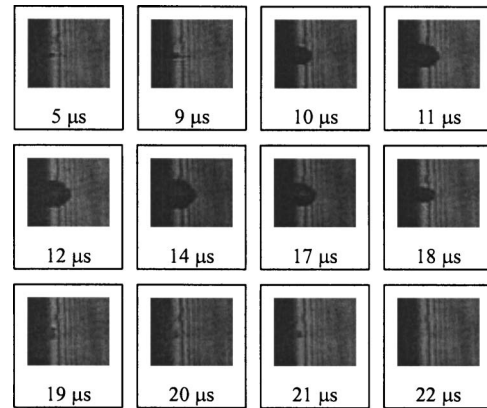


Figure 6. Shadowgraphs of bubbles at various delay times (Ar ion laser pulse width: 9 μs, laser power: 500 mW). The image (horizontal) size is 220 μm.

are presented with ±8% uncertainty, which comes from the volume calculation in the image processing. The line in Fig. 7 represents fitting by the Gaussian peak curve. It is shown that the bubble lifetime is approximately 10 μs. Analysis of the data also reveals that initial growth of the bubble approximates to $r \sim t^{0.5}$, where r and t represent bubble radius and time, respectively. Noting that the bubble in the heat transfer controlled regime is proportional to the square root of time,¹⁷ it can be claimed that the heat flux is not sufficient to induce linear growth of the bubble in the inertia controlled stage. Accordingly, further reduction of the bubble incipience time is expected in the case of higher power laser irradiation. The collapse of a bubble has been found to be similar to that of a typical cavitation bubble. Spherical shock waves are observed when the bubble collapses. The time t_{col} required for the bubble to collapse is given by;¹⁸

$$t_{col} = 0.915R_{max} \left[\frac{\rho_l}{p_{amb} - p_{sat}(T_{amb})} \right]^{1/2}, \quad (1)$$

where R_{max} is maximum bubble radius, ρ_l is liquid density, p_{amb} is ambient pressure, T_{amb} is ambient temperature, and

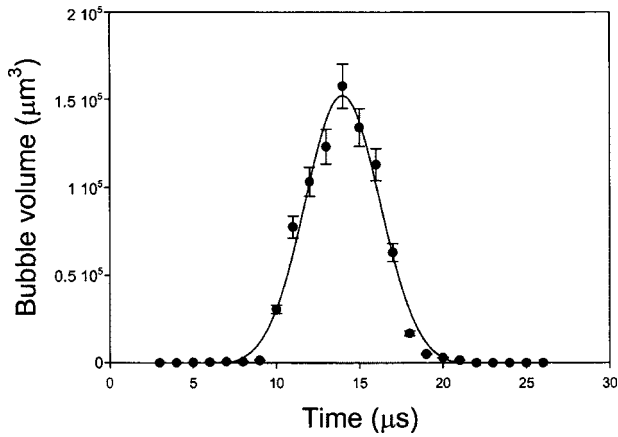


Figure 7. Variation of bubble volume with time for a typical heating condition: Laser power 500 mW, pulse width 9 μ s, 33% volume concentration (magenta).

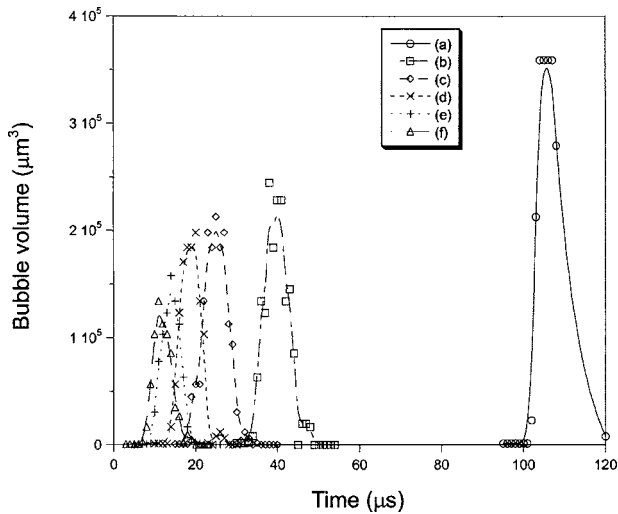


Figure 8. Variation of bubble volume with time: (a) Ar ion laser power=100 mW, pulse width=105 μ s, (b) 200 mW, 35 μ s, (c) 300 mW, 20 μ s, (d) 400 mW, 14 μ s, (e) 500 mW, 9 μ s, and (f) 610 mW, 7 μ s. Bubbles are generated in the ink solution (33% volume concentration).

p_{sat} is saturation pressure. According to Eq. (1), the collapse time is $\sim 5 \mu$ s for typical experimental conditions, where $R_{max}=50 \mu$ m, $\rho_l=1000 \text{ kg/m}^3$, $p_{amb}=100 \text{ kPa}$, $T_{amb}=300 \text{ K}$, $p_{sat}(T_{amb})=3.1691 \text{ kPa}$. The generated bubbles are approximately 100 μ m in diameter in typical cases and their collapse times are 5–10 μ s, which is consistent with the theoretical prediction using Eq. (1).

EFFECT OF LASER POWER

The bubble dynamics, including the incipience time, bubble size, and volume, have been measured by varying the laser power. Figure 8 exhibits the temporal variation of the bubble volume for various laser powers and pulse widths. The figure reveals that both the boiling incipience time and the maximum bubble volume decrease with the laser power. Note that the laser pulse width has been adjusted to a minimum value that provides the threshold pulse energy required for

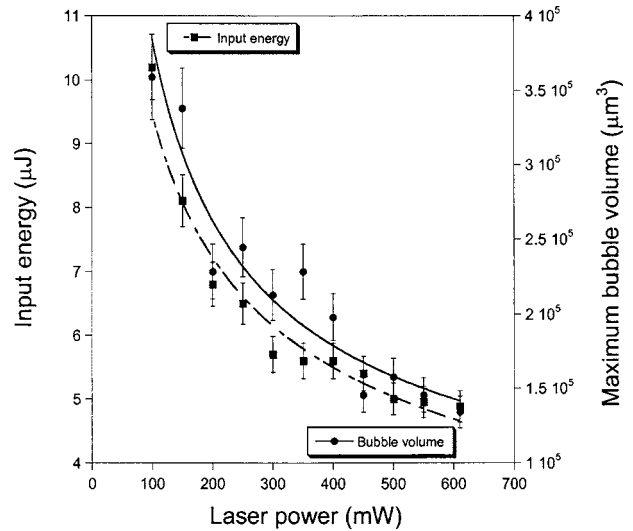


Figure 9. Minimum energy for bubble inception and the maximum bubble volume for various laser powers.

boiling incipience. In other words, the laser beam is cutoff after the time to explosive bubble formation. Figure 8 also indicates that the behavior of the laser produced bubble is largely similar to that generated by a thin film heater in a typical ink jet device,^{8–10} with similar time scales for bubble growth and collapse. For example, in the boiling experiment of methanol by an electrical thin film heater,⁹ heating time and bubble lifetime were approximately 5 and 10 μ s, respectively, (when input energy=3 μ J, maximum bubble radius=70 μ m, and heat flux= $5.1 \times 10^3 \text{ W/cm}^2$).

The effect of laser power on the minimum energy for bubble incipience and the maximum bubble volume is shown in Fig. 9. The measured data are shown with $\pm 8\%$ and $\pm 5\%$ uncertainties for maximum bubble volume and input energy, respectively. The error for maximum bubble volume originates from the determination of bubble radius in the shadowgraphy image processing. The input energy is calculated by multiplying the laser power by the pulse width, i.e., the boiling incipience time. The pulse width fluctuates in the range of $\pm 5\%$ and serves as the main source of uncertainty. When the laser power is changed from 100 to 610 mW, the minimum energy for boiling incipience and maximum bubble volume decrease from 10 to 5 μ J and from 3.5 to $1.5 \times 10^5 \mu\text{m}^3$, respectively. Figure 9 reveals that the maximum bubble volume decreases with laser power, which is to be respected because of the reduced boiling incipience time.

The effect of heat flux q on the boiling incipience has been investigated. It is assumed that the beam profile has a Gaussian spatial distribution with a spot size of 26 μ m (theoretically estimated diameter) at the interface between the ink solution and the window. The boiling incipience time decreases with the heat flux and is shown to be proportional to $q^{-1.39}$ (Fig. 10). These results suggest that high power laser irradiation could lead to rapid bubble generation on a time scale of a few microseconds. It is evident that the exponent -1.39 would be further lowered if the power or the

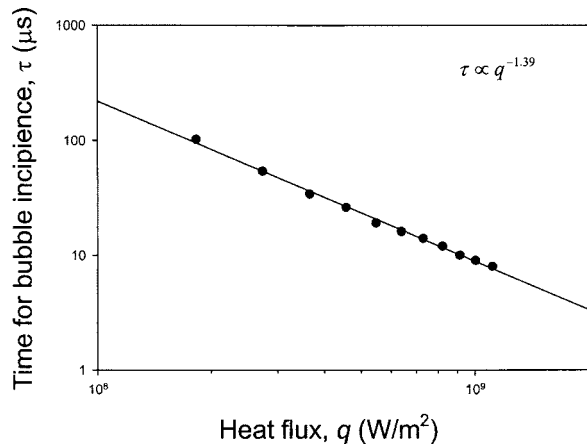


Figure 10. Effect of heat flux on bubble incipience time.

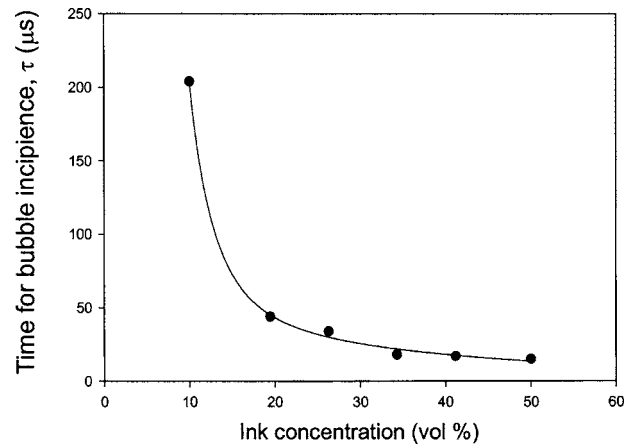


Figure 11. Bubble incipience time for various ink concentrations for magenta ink.

absorption is increased. According to Asai's calculation,¹⁰ stronger dependence of τ on q can be obtained. For example, a dependence $q^{-1.99}$ has been reported in the case of heating by a thin film heater. The thermal energy released by a heater is confined in the heat-affect zone with a diffusion length scale l_t

$$l_t \sim \sqrt{\alpha t_0} = 0.9 \mu\text{m}, \quad (2)$$

where α and t_0 represent the thermal diffusivity and the heating time. On the other hand, in the present case, the laser pulse energy is confined in the optical penetration zone with a length scale l_o

$$l_o \sim \frac{1}{\kappa} = 91 \mu\text{m}, \quad (3)$$

where κ is absorption coefficient for the 33% ink solution. Therefore, the heating efficiency, i.e., the rate of temperature increase, is relatively low since the optical penetration depth is longer than the thermal penetration depth. It is pointed out again that dilute ink solutions are used for the purpose of visualization, reducing the absorption coefficient on purpose. Consequently, the lowered heating efficiency by enlarged optical penetration depth can explain the relatively weak dependence of τ and q .

EFFECT OF INK CONCENTRATION

As mentioned above, the ink concentration is an important parameter in the laser-induced bubble generation. When the concentration of the ink solution is changed, its light absorption property varies significantly as displayed in Fig. 4. The boiling incipience time is exhibited in Fig. 11 for various concentrations of magenta ink. The boiling incipience time decreases as the ink concentration increases, which is because the high concentration solution strongly absorbs the laser energy. In Fig. 11, the results for concentrations higher than 50% are missing since the probe laser beam does not transmit through the ink solution in the range, making the bubble visualization impossible. To examine the dependence of the laser induced bubble dynamics on color of the ink,

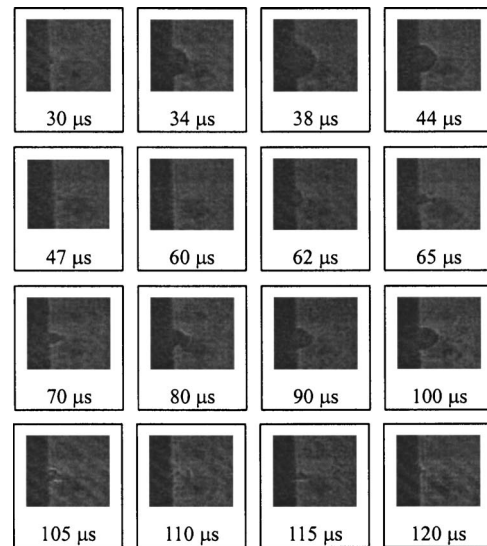


Figure 12. Shadowgraphs of bubbles at various delay times (Ar ion laser pulse width: 100 μs, laser power: 605 mW). The image (horizontal) size is 220 μm.

similar experiments have been carried out using the yellow color. Strong concentration dependence is observed in the case of yellow ink as well. While the boiling incipience time for the magenta ink is approximately 15 μs at a volume concentration of 50% (laser power=270 mW), the boiling incipience time for the yellow ink is 90 and 20 μs for volume concentrations 41% and 100%, respectively.

EFFECT OF LASER PULSE WIDTH

Experiments for visualizing the bubble dynamics were performed for various laser pulse widths. Figure 12 displays the temporal variation of the bubble shape for a laser pulse of 100 μs. In this experiment, the boiling incipience time and maximum bubble size are larger than that shown in the previous section (Fig. 7), because the laser spot is bigger by approximately 40%. As shown in Fig. 13(a), when the laser pulse width slightly exceeds the incipience time (about

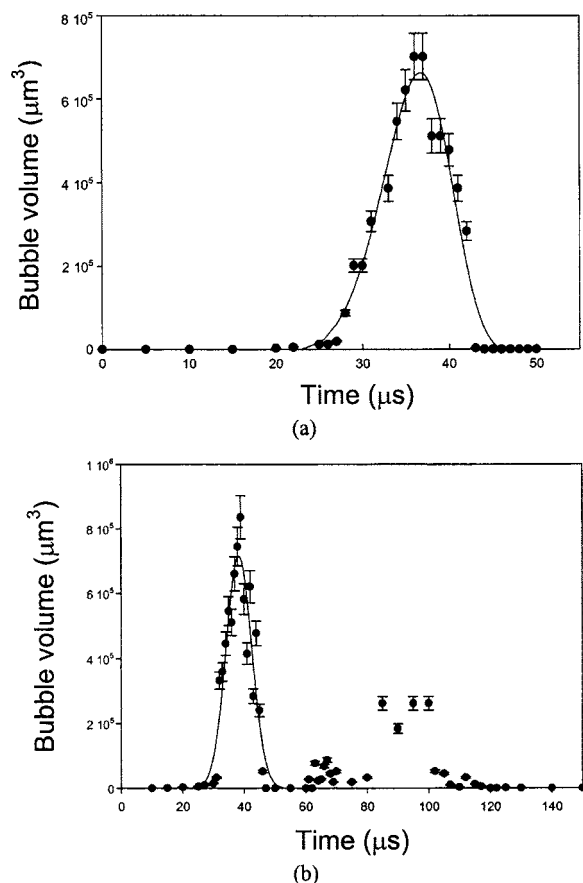


Figure 13. Variation of bubble volume with time for a typical heating condition: Laser power 605 mW, pulse width (a) 27 μs and (b) 100 μs , 50% volume concentration (magenta).

0.5–1 μs), a relatively large single bubble is generated. On the other hand, if the laser pulse significantly longer than the bubble incipience time [Fig. 13(b)], the initially created bubble collapses during the laser pulse without continued growth and the bubble growth and collapse are repeated until the end of the pulse. It is notable that, even for a laser pulse longer than τ , the behavior of the initially formed bubble, including the incipience time, collapse time, maximum bubble size, and growth rates, does not vary significantly with the pulse width. The dynamics of the initially appearing bubble is similar in all cases regardless of the irradiation time as plotted in Fig. 14. It is shown that this saturation behavior with the incident laser energy is due to the instability related with the optical energy coupling into the liquid. As the bubble grows, the liquid-vapor interface recedes from the original position, i.e., from the focal plane. Therefore, the laser beam is gradually defocused and the bubble eventually blocks the energy input for further growth. The laser spot size is an important parameter that governs the laser induced bubble dynamics as it determines the heat flux. Furthermore, the position of the focal plane relative to the inner surface of the quartz window (d in Fig. 15) is critical as the absorption plane (ink-bubble interface) moves during the bubble lift time. Figure 15 indicates that the bubble growth by a laser beam is self-limited by the

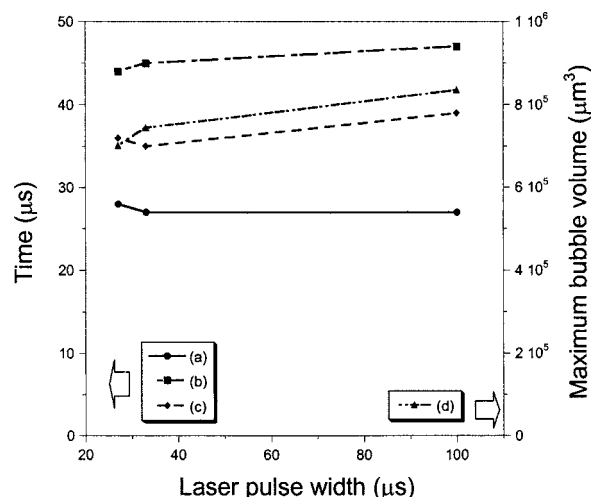


Figure 14. Dependence of bubble characteristics for various laser pulse widths (ink concentration=50% by volume, laser power=610 mW): (a) Bubble incipience time, (b) bubble collapse time, (c) time to reach the maximum bubble size, and (d) maximum bubble volume.

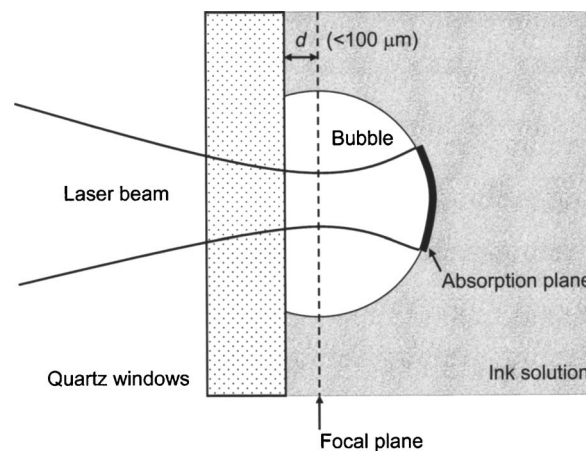


Figure 15. Bubble formation on the quartz window by the Ar ion laser beam.

defocusing effect. Once the bubble is larger than a certain size, the heat flux, i.e., irradiation, becomes too low to provide the bubble with sufficient momentum for growth. Also, Fig. 15 suggests that there should be an optimal location of the focal plane in view of minimizing the boiling incipience time. As mentioned earlier, this optimal position was found by adjusting the d value using a micrometer stage. However, the optimal value, which is smaller than 100 μm , could not be quantified since it was difficult to locate the absolute position of the focal plane, precisely. The bubble incipience time τ changes up to 20 μs as the distance d is varied by approximately 100 μm .

BUBBLE DYNAMICS BY MULTIPLE LASER PULSES

To examine the effect of successive laser pulses, the bubble dynamics have been analyzed for double pulse conditions. Figure 16 illustrates the bubble dynamics induced by two successive laser pulses. It is shown that the behavior of the initially appearing bubble is similar to that in the case of a

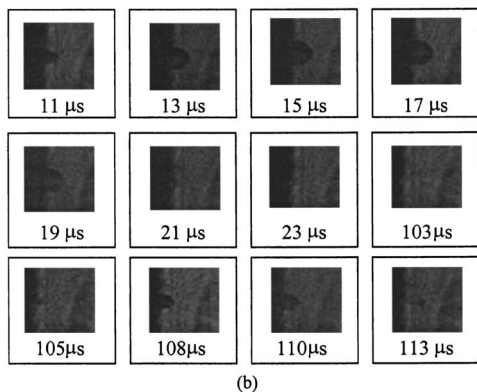
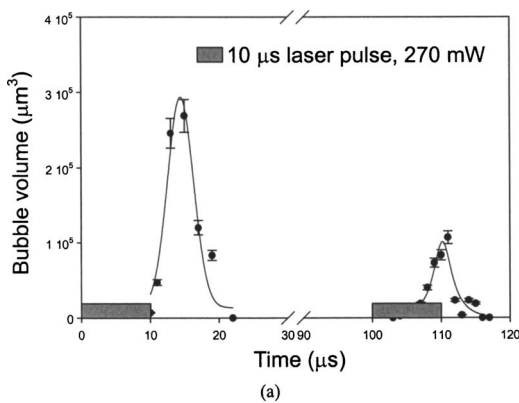


Figure 16. Bubble generation by double laser pulses: (a) Variation of bubble volume with time, and (b) bubble images at various delay times (interval between two laser pulses=100 μ s).

single pulse case. However, the second bubble that appears after the collapse of the first bubble has substantially different characteristics. The maximum volume of the second bubble is considerably smaller compared to the first bubble. Furthermore, the time for the second bubble incipience is much shorter than that of the initially appearing bubble, indicating a possibility of high frequency bubble generation. However, it has also been observed that the second bubble becomes less stable than the first one as the delay between the two laser pulses is reduced, i.e., the shape is relatively irregular and fluctuating. This instability of the second bubble formation for short pulse-to-pulse intervals is believed to be due to incomplete cooling of the liquid and also to the bubble nuclei remaining even after the first bubble collapse. Despite the increased instability of the bubble formation, it is apparent that the characteristic time for the second bubble incipience can be reduced in the case of successive irradiation of laser pulses. It is noted that the instability problem would be less important in the case of operation of a real ink jet printer head as the droplet removes a significant portion of the thermal energy released by the preceding laser pulse when the droplet is ejected through the nozzle.

CONCLUSIONS

This work reports, for the first time to our knowledge, the details of the bubble dynamics induced by pulsed laser heat-

ing of absorbing liquid in contact with a transparent solid surface in range of the power density $O(10^4 \text{ W/cm}^2) \sim O(10^5 \text{ W/cm}^2)$. Measurement of absorption spectrum revealed that a commercial ink has a strong absorption band in the wavelength range from 400 to 500 nm. The experimental results indicate that the direct laser-pulse (pulse energy $\sim 5 \mu\text{J}$) heating of absorbing liquids enables the generation of rapidly growing/collapsing bubbles with a lifetime of $\sim 10 \mu\text{s}$. It has been found that the characteristics of the laser generated bubble are largely similar to those produced by conventional thin film heaters. However, there are some unique features of optical heating, e.g., saturation of bubble growth with the laser pulse width and strong dependence of the phenomena on the position of the focal-plane and on ink color and concentration. This work demonstrates the technical feasibility of developing a novel laser based droplet generation mechanism for applications in ink jet printer heads, though further research needs to be done for quantitative assessment of their effectiveness.

ACKNOWLEDGMENTS

This work was supported by grant no. R01-2005-000-10658-0 from the Basic Research Program of the Korea Science & Engineering Foundation and by Micro Thermal System ERC.

REFERENCES

- S. N. Maximovsky and G. A. Radutsky, U.S. Patent No. 6,056,388 (2000).
- S. N. Maximovsky and G. A. Radutsky, U.S. Patent No. 6,231,162 B1 (2001).
- S. N. Maximovsky and G. A. Radutsky, U.S. Patent No. 6,270,194 B1 (2001).
- S. N. Maximovsky and G. A. Radutsky, U.S. Patent No. 6,330,857 (2001).
- K. Nemoto, O. Matsuda, and M. Doi, U.S. Patent No. 5,713,673 (1998).
- I. Endo, Y. Sato, S. Saito, T. Nakagiri, and S. Ohno, U.S. Patent No. 4,723,129 (1988).
- M. Kohyama, U.S. Patent No. 5,021,808 (1991).
- A. Asai, T. Hara, and I. Endo, "One-dimensional model of bubble growth and liquid flow in bubble jet printers", *Jpn. J. Appl. Phys., Part 1* **26**, 1794 (1987).
- A. Asai, "Bubble dynamics in boiling under high heat flux pulse heating", *ASME Trans. J. Heat Transfer* **113**, 973 (1991).
- A. Asai, "Application of the nucleation theory to the design of bubble jet printers", *Jpn. J. Appl. Phys., Part 1* **28**, 909 (1989).
- D. Kim, M. Ye, and C. P. Grigoropoulos, "Pulsed laser induced ablation of absorbing liquids and acoustic-transient generation", *Appl. Phys. A* **67**, 169 (1998).
- H. Shanguan, L. W. Casperson, D. L. Paisley, and S. A. Prah, "Photographic studies of laser-induced bubble formation in absorbing liquids and on submerged targets: implications for drug delivery with microsecond laser pulses", *Opt. Eng.* **37**, 2217 (1998).
- I. Turovets, D. Palanker, Y. Kokotov, I. Hemo, and A. Lewis, "Dynamics of cavitation bubble induced by 193 nm ArF excimer laser in concentrated sodium chloride solutions", *J. Appl. Phys.* **79**, 2689 (1996).
- Y. Tomita, A. Shima, and K. Sato, "Dynamic behavior of two-laser-induced bubbles in water", *Appl. Phys. Lett.* **57**, 234 (1990).
- B. Ward and D. C. Emmony, "Conservation of energy in the oscillations of laser-induced cavitation bubbles", *J. Acoust. Soc. Am.* **88**, 434 (1990).
- A. Vogel, W. Lauterborn, and R. Timm, "Optical and acoustic investigations of the dynamics of Laser-produced cavitation bubbles near a solid boundary", *J. Fluid Mech.* **206**, 299 (1989).
- V. P. Carey, *Liquid-Vapor Phase-Change Phenomena* (Hemisphere, Washington, D.C., 1992), p. 192.
- R. Rayleigh, "On the pressure developed in a liquid during the collapse of a spherical cavity", *Philos. Mag.* **34**, 94 (1917).